

Geophysical Research Letters[®]

RESEARCH LETTER

10.1029/2022GL100474

Key Points:

- Plate bending at the transition from the Manila subduction zone to the Taiwan collision zone was simulated by a 3-D flexural model
- High value of plate bending stress in simulation is consistent with the concentrated seismic activity at southwest of the Taiwan
- We proposed a concept model to illustrate plate bending and seismicity at the transition from subduction to collision

Supporting Information:

Supporting Information may be found in the online version of this article.

Correspondence to:

Z. Sun and H. Yang,
zhensun@scsio.ac.cn;
hyang@cuhk.edu.hk

Citation:

Zhang, J., Sun, Z., Yang, H., & Zhang, F. (2022). A model of plate bending at the transition zone from subduction to collision in northernmost Manila trench. *Geophysical Research Letters*, 49, e2022GL100474. <https://doi.org/10.1029/2022GL100474>

Received 15 JUL 2022

Accepted 1 SEP 2022

A Model of Plate Bending at the Transition Zone From Subduction to Collision in Northernmost Manila Trench

Jiangyang Zhang^{1,2} , Zhen Sun^{1,2} , Hongfeng Yang³ , and Fan Zhang^{1,2} 

¹Key Laboratory of Ocean and Marginal Sea Geology, South China Sea Institute of Oceanology, Chinese Academy of Sciences, Guangzhou, China, ²Southern Marine Science and Engineering Guangdong Laboratory (Guangzhou), Guangzhou, China, ³Earth System Science Programme, Faculty of Science, the Chinese University of Hong Kong, Shatin, China

Abstract It is not rare to observe subduction zones transferring into collision zones. However, it is poorly understood the lateral variation in flexural deformation. Constrained by newly published seismic reflection data, we investigate the mechanical behavior of lithosphere from oceanic subduction to collision at the northern Manila trench using the 3-D flexural modeling. Results show that both plate rigidity and the loadings increase from the Manila subduction zone to the Taiwan orogenic belt. In order to fit all observations, an upward loading was required at the transition zone from subduction to collision, which may be related to the variation of buoyancy due to density contrast of plate from south to north. The resultant maximum bending stress is consistent with the concentrated seismic activity at the southwest of Taiwan, suggesting that huge loading from the orogeny and lateral density change of subducting plate play important roles in bending and seismicity.

Plain Language Summary Converge of two plates forms the subduction zone and collision zone, causing great bending of lithosphere. Faulting and earthquakes may be induced by plate bending when the deformation exceeds strength limit of lithosphere. Here, the flexural of the subducting plate along the northernmost Manila trench has been simulated by a 3D model. Results show that from subduction to collision, both surface loading coming from mountain belt and buoyancy difference between oceanic and continental plate play critical roles in plate bending. The results also reveal that the buoyancy difference due to density contrast between the oceanic and continental plate may generate an upward loading at the transition zone from subduction to collision. Concentrated intraplate seismic activity at depth of ~50 km is consistent with the maximum value of simulated bending stress and we finally proposed a concept model to illustrate plate bending and seismicity at the transition from subduction to collision.

1. Introduction

Both subduction and collision zone have long been recognized as the convergent boundaries of tectonic plates where the lithospheric flexural deformation occurs. Along strike, subduction zones may pass into collision zones, such as the Sumatra-Java subduction zone that transferred to the East Java continent-arc collision zone along with the arrival of Australia (Silver et al., 1983), the Manila subduction zone transferred northward into the Taiwan collision zone (Huang et al., 2000). This process holds significant implications to the study of the mechanical behavior of the subducted plate, including the bending stress and the distribution of the bending-related earthquakes (Hunter & Watts, 2016; Judge & McNutt, 1991; Levitt & Sandwell, 1995; Watts, 2001; Zhang et al., 2014, 2021; Zhou et al., 2015).

Plate bending has been widely investigated in the Manila subduction zone (Chang, Yu, Hsu, & Liu, 2012; Chang, Yu, Lee, et al., 2012) and the West Taiwan Foreland Basin (Chang, Yu, Hsu, & Liu, 2012; Chang, Yu, Lee, et al., 2012; Chou & Yu, 2002; Lin et al., 2003; Lin & Watts, 2002; Mouthereau & Petit, 2003; Tensi et al., 2006), respectively. Based on a comprehensive analysis of the seismic and well data, Lin & Watts (2002) modeled the bending shape of the West Taiwan Basin with a 2-D thin elastic plate model and found that the best-fitting T_e is 13 km. Mouthereau and Petit (2003) modeled the plate flexure of the West Taiwan Basin with brittle-elastic-ductile plate rheology. The results showed that T_e varied in the range of ~15–20 km. Tensi et al. (2006) investigated the timing and the origin of the lithospheric bulge in the West Taiwan Basin using well data. They gave the calculated T_e with 10–20 km. Based on analysis of bathymetry, gravity, and seismic data, Chang, Yu, Hsu, and Liu (2012); Chang, Yu, Lee, et al. (2012) studied the characteristics of the outer rise seaward of the Manila trench and indicated that T_e of the subducting plate was in the range of 13–16 km. Most previous studies used a 2-D

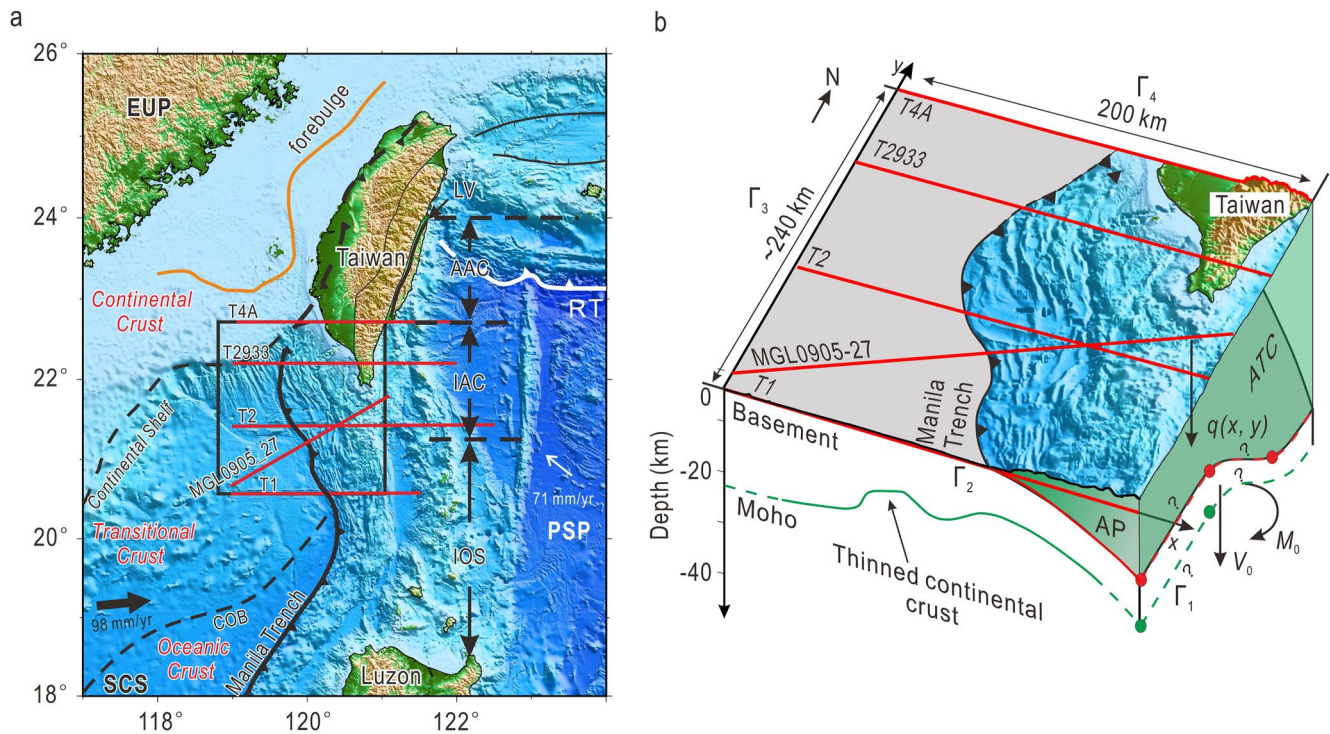


Figure 1. Crust structure of the northern Manila trench and Taiwan collision zone. (a) Tectonic setting of the study area and the location of seismic profiles. Dashed lines represent continental shelf and Continent Ocean Boundary, which divide the subducted plate into continental, transitional and oceanic crust. The orange line is the edge of forebulge from Lin and Watts (2002). EUP—Eurasian Plate; PSP—Philippine Sea Plate; LV—Longitudinal Valley; RT—Ryukyu Trench; IOS—Intra-oceanic Subduction; IAC - Initial Arc-continent Collision and AAC—Advanced Arc-continent Collision (from Huang et al., 2000). The convergence rates and direction along the Manila trench are from Rangin et al. (1999) and Seno et al. (1993). (b) Schematic diagram of our 3-D flexural models constructed by the seismic profiles. The size of the model is corresponding with the black rectangle in Figure 1. Both bending moment ($-M_0$) and shear force ($-V_0$) are vectors. $T_e(x, y)$ and $q(x, y)$ are effective elastic thickness and surface loading which are allowed to vary spatially. AP: Accretionary prism; ATC: Accreted transitional crust. The basement (red lines) and Moho (green lines) are based on previous published profiles (Eakin et al., 2014; Lester et al., 2013; McIntosh et al., 2013).

thin plate model focused on trench-normal deformation but ignored lateral variation along the subduction zone. Moreover, the 2-D model implicitly assumes that the lithospheric flexure is caused entirely by the drag of the down-going slab. This assumption does not apply to the transition from subduction to collision, as the greater dragging force from the lateral plate caused by huge surface loading (mountain belt) may play a critical role in plate bending. Furthermore, in 2-D models, the plate is always assumed to be continuous and elastic along the subduction zone. Lateral slab tears or inelastic deformations may not be recognizable in 2-D models. Therefore, 3-D models of plate bending at the transition from subduction to the collision are demanded to reveal more realistic deformation features of the down-going plate.

With the new published wide-angle seismic data acquired offshore Taiwan (Eakin et al., 2014; Lester et al., 2013; McIntosh et al., 2013), the northernmost Manila trench is therefore an ideal place to study the plate flexural deformation from subduction zone to collision environment. In this study, we first construct a bending surface with the seismic data. Constrained by seismic profiles, a 3-D thin plate bending model, with the lateral changes in lithospheric parameters such as the effective elastic thickness (T_e), surface loading and boundary loading, was used to simulate the bending morphology from the Manila trench to Taiwan collision zone. Then we calculated the bending stress of subducted plate and discussed their relationship with the distribution of the intra-plate earthquakes. Finally, we proposed a model to illustrate the effects of upper plate on plate bending in the transition zone from subduction to collision.

2. Geological Setting

The interactions between the Eurasian Plate and the Philippine Sea Plate have resulted in the magnificent Taiwan Island (Figure 1a). In the northeastern South China Sea (SCS), the convergent belt experienced a

transition from a subduction in the south (Manila trench) to an arc-continent collision in the north (Taiwan). The Manila trench, located at the east of the SCS, was formed by the subduction of the Eurasian Plate beneath the Philippine Sea Plate (Bowin et al., 1978; Hayes & Lewis, 1984; Taylor & Hayes, 1983; Yu & Kuo, 1999) at the Middle Miocene (Wolfe, 1988) or at the Late Oligocene (Hayes & Lewis, 1984; Wang & Li, 2009). Huang et al. (2000) pointed out that the Taiwan arc-continent collision could be divided into four geodynamic processes: Intro-oceanic subduction (south of 21°20' N), Initial arc—continent collision (21°20' N—22°40' N), Advanced arc—continent collision (22°40' N—24°N), and Arc collapse/subduction (24°N—24°30' N).

From the arc-continent collision (north) to the subduction zone (south), both properties and thickness of the subducting crust vary along the strike (Kuo-Chen et al., 2012; Ludwig et al., 1967; McIntosh et al., 2005). On Taiwan Island, the thickness of the continental crust in the west of Taiwan is ~26 km, but up to ~55 km beneath central Taiwan (Van Avendonk et al., 2014). The crustal thickness in the south of Taiwan (~22.7°N, T4A in Figure 1a) is ~9–15 km (McIntosh et al., 2013). At the Hengchun Peninsula of southernmost Taiwan, ~11-km-thick, transitional crust of the Eurasian Plate was subducted beneath a vast, rapidly growing accretionary prism (T2933 in Figure 1a) (McIntosh et al., 2005). Further south, at the area between ~21.5 and ~22.5°N, The crustal structure showed characteristics of an incipient mountain belt at the earliest stage of arc-continent collision (MGL0905_27 in Figure 1a and Figure S1e in Supporting Information S1). The 1D velocity model suggested that the velocity structure of the crust near the trench is consistent with the continental crust of the distal Chinese continental margin. The distal margin crust was 10–14 km thick near the trench but thins to 6 km thick beneath the lower slope (Lester et al., 2013). It means that normal oceanic crust has been subducted beneath the thick accretionary prism. The Multi-Channel Seismic profile showed that the subduction of normal ocean crust might occur at the south of ~22°N (Eakin et al., 2014). (All profiles of crust structure are displayed in Figure S1 of Supporting Information S1).

These profiles of velocity structure suggested that from south to north, the tectonic setting changed from the Manila trench to Taiwan arc-continent collision zone. The crust of the Eurasian Plate varied from oceanic crust to transitional crust, then to continent crust, with the crust thickness increasing. Although the relation between T_c and the thickness of the crust is still controversial, the morphology of basement along these profiles could help us constrain the plate bending model. Because compared to bathymetry profiles, seismic profiles reflect the “real” deformation of the plates and avoid the interferences of sediments, especially in the area with thick deposit.

3. Numerical Modeling

3.1. Plate Bending

As variable T_c , surface ($q(x, y)$ from the overriding wedge) and boundary loadings (the bending moment M_0 and the vertical shear force V_0) need to be overcome during plate subducting, we use the finite difference method (FDM) to simulate the flexural deformation of a 3-D subducted plate (Zhang, Sun et al., 2018; Zhang et al., 2021) (Please see the Text S1 in Supporting Information S1).

Although the material in our modeling is elastic, the variable T_c supports us to investigate the geometric shape of lithospheric inelastic deformation (Contreras-Reyes & Osses, 2010). In our model, the reduction in T_c is regarded as the plastic deformation after yielding due to plate weakening caused by strong bending near the trench axis. Contreras-Reyes and Osses (2010) pointed out that the observed bending-related faults, low P wave velocity of the mantle and short flexural wavelength at the outer rise of the Chile trench demonstrated the plate hydration and weakening at the area close to subduction zones. In our study area, we believed that widely distributed bending-related faults and intraplate earthquakes also support the plate weakening and reduction in T_c . The change of crustal thickness from south to north (ocean to land) would cause lateral differences of both plate buoyancy and mechanism state. In our model, this discrepancy can be reflected by the lateral variation in boundary loadings (Please see the Text S1 in Supporting Information S1).

The computational domain is a rectangle between T1 and T4A profiles (Figure 1b) with a width of ~240 km (along the strike of the Manila trench) and the length of 200 km (perpendicular to the trench). The east boundary is a stretch of the Longitudinal Valley (LV in Figure 1a) to south, representing the boundary between the Eurasian Plate and the Philippine Sea Plate (Wang & Lee, 2011). In order to avoid edge effects, the lengths of our models

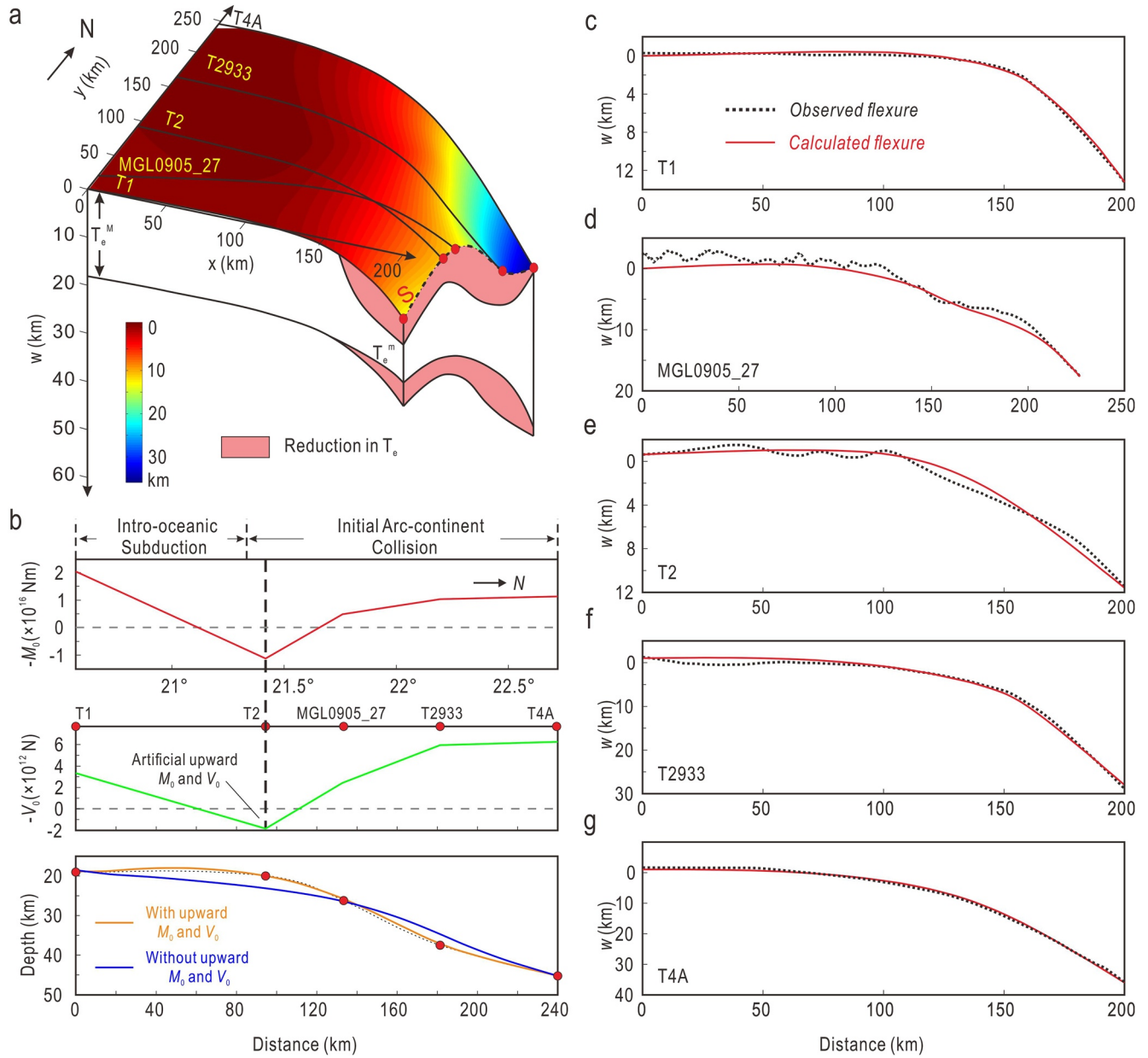


Figure 2. (a) 3-D simulated result, the red part represent the reduction in the effective elastic thickness (T_e); (b) Inverted boundary bending moment ($-M_0$), vertical force ($-V_0$) and the bending morphology along the S in Figure (a). (c–g) The comparison between our model and the observed data.

have been reasonably extended westward (400 km long), similar to Wang & Lee, (2011). The boundary conditions are (Figure 2b and Figure S2 in Supporting Information S1):

$$\begin{aligned}
 \Gamma_1 : \bar{M}_y &= -\bar{M}_0, \bar{V}_y = -\bar{V}_0 \\
 \Gamma_2 : M_x &= 0, V_x = 0 \\
 \Gamma_3 : w &= 0, M_x = 0 \\
 \Gamma_4 : M_x &= 0, V_x = 0
 \end{aligned}
 \tag{1}$$

Here the $M_0(y)$ is the bending moment and $V_0(y)$ is the boundary vertical shear force. They are both vectors and may vary along trench.

Using the basement morphologies of the five profiles (T1, MGL0905–27, T2, T2933, and T4A), a 3-D morphology of the flexural plate has been constructed by interpolation method (Figure 1b). We constrained our model

by minimizing the root mean square error of flexure $W_{\text{RMS}}(m) = \sqrt{\frac{1}{n} \sum_{i=0}^n |w_i(m) - d_i|^2}$ between the calculated flexure $w(m)$ and the observed data d_i , where n is the number of nodes along the modeled profiles. As there are so many inversion parameters for conventional analysis, parameter vectors are searched by particle swarm optimization (PSO) inversion method (Shi & Eberhart, 1998; Zhang et al., 2021) (Please see the Text S2 in Supporting Information S1).

3.2. Distribution of Bending Stress

Once the plate bending w was obtained, the components of plane stresses can be derived by (Turcotte & Schubert, 2014):

$$\begin{bmatrix} \sigma_{xx} \\ \sigma_{yy} \\ \sigma_{xy} \end{bmatrix} = -\frac{Ez}{1+\mu} \begin{bmatrix} \frac{1}{1-\mu} & \frac{\mu}{1-\mu} & 0 \\ \frac{\mu}{1-\mu} & \frac{1}{1-\mu} & 0 \\ 0 & 0 & 1 \end{bmatrix} \begin{bmatrix} \frac{\partial^2 w}{\partial x^2} \\ \frac{\partial^2 w}{\partial y^2} \\ \frac{\partial^2 w}{\partial x \partial y} \end{bmatrix} \quad (2)$$

where z is the distance from the neutral plane. x and y are directions normal and parallel to the subduction-collision zone, respectively. When we discuss the bending stress, the stress components should be projected onto the horizontal coordinate axis along the direction of maximum curvature (Garcia et al., 2019), with the following principal stresses (the maximum principal stress σ_1 and the minimum principal stress σ_2):

$$\begin{aligned} \sigma_1 &= \frac{\sigma_{11} + \sigma_{22}}{2} + \sqrt{\left(\frac{\sigma_{11} - \sigma_{22}}{2}\right)^2 + \sigma_{12}^2} \\ \sigma_2 &= \frac{\sigma_{11} + \sigma_{22}}{2} - \sqrt{\left(\frac{\sigma_{11} - \sigma_{22}}{2}\right)^2 + \sigma_{12}^2} \end{aligned} \quad (3)$$

4. Results

Constrained by the newly acquired wide-angle seismic data, a 3-D flexural model of northern Manila subducted plate simultaneously fitting all observations was obtained (Figures 2a, 2c and 2g and Figure S3a in Supporting Information S1). The W_{RMS} between the model and the observation is ~ 0.47 km (Figure S3b in Supporting Information S1). The $q(x, y)$ increases northward from $\sim -1.6 \times 10^8$ N to $\sim -7.9 \times 10^8$ N (Figure S3c in Supporting Information S1). Our inversion results show that from oceanic (south) to continental lithosphere (north), the T_e^{M} changes from 19 to 33 km and the T_e^{m} changes from 7 to 26 km (Figure 2a and Figure S3d in Supporting Information S1). From the subduction to collision zone, the bending moment $-M_0$ increases from 0.9×10^{16} to 2.02×10^{16} Nm and the boundary vertical force $-V_0$ changes from 3.35×10^{12} to 6.25×10^{12} N. These values are similar to that of previous trench-bending models (Contreras-Reyes & Osses, 2010). In order to fit the along-strike variation of plate deflection, both $-M_0$ and $-V_0$ are upward at $\sim 21^\circ 30' \text{N}$ corresponding to the transition zone from the Intra-oceanic Subduction (IOS) to Initial Arc-continent Collision (IAC). Figure 3 displays the variation of plate bending stress, with the red color representing extensional stress and the blue color representing compressional stress. The bending stress increases from subduction to collision zone and reach the maximum to the southwest of the Taiwan Island (Figure 3).

Seismic events from the International Seismological Centre (black dots in Figure 3b) and the Global Centroid Moment Tensor ($M_w > 4$) are displayed in the Figure 3b and projected on two profiles (Figures 3c and 3d). The results show that earthquakes are concentrated in the southwest of the Taiwan Island with depths 35–50 km.

5. Discussion

5.1. Along-Strike Variation of T_e in Northernmost Manila Trench

Compared with previous studies, the T_e^{M} in our study is slightly higher than those previous ones, potentially due to three reasons. One is that most of the former researches only took into account of surface loading (accretionary wedge and orogenic belt), and did not consider the boundary loading M_0 and V_0 (Lin et al., 2003; Lin &

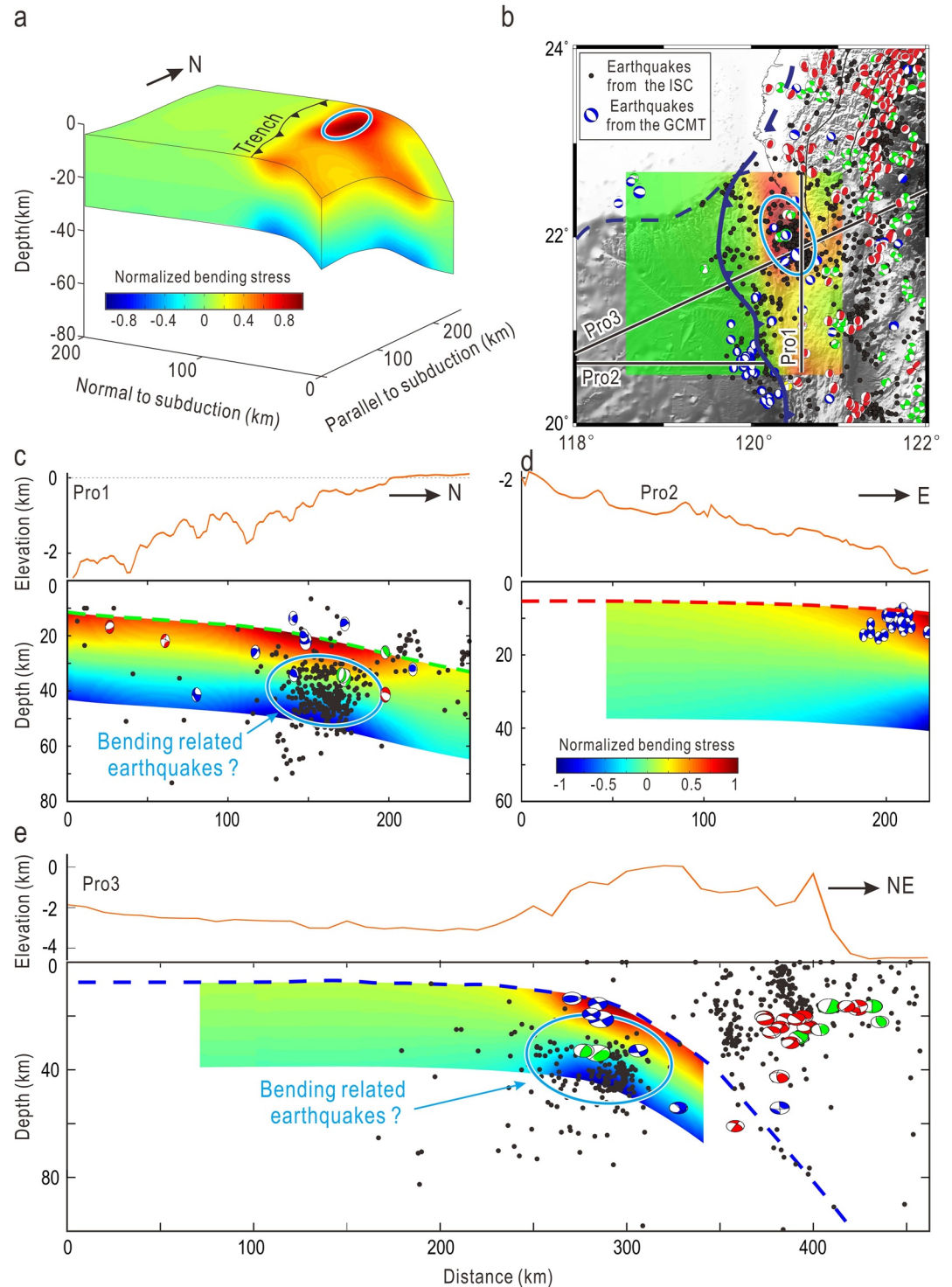


Figure 3. (a) 3-D maximum principle bending stress. The orange ellipse represents the place where the intraplate earthquakes are concentrated; (b) The seismicity of the study area. The black dots represent the earthquakes from the ISC catalog; The focal mechanisms are from Global Centroid Moment Tensor (GCMT) ($M_w > 4.0$) (c) Bending stress and seismicity profile along the Profile one in Figure (b). The color of bending stress is the same as that in panel (a). (d) Bending stress and seismicity profile along the Profile two in Figure (b). Please note that the color bar here is only for panel (d). (e) Bending stress and seismicity profile along the Profile three in Figure (b). The color of bending stress is the same as that in panel (a).

Watts, 2002; Mouthereau & Petit, 2003; Tensi et al., 2006). However geophysical observations show that even in the orogenic belt, the pull or flattening of deep subducted slab has a great effect on plate bending and distribution of seismicity, such as the Tibetan plateau (Liang et al., 2012) and Anatolia (Govers & Fichtner, 2016). Ignoring M_0 and V_0 may cause an underestimate of T_c . The second reason is that most previous work used a 2-D model. This would bring deviation in estimating flexural parameters (Zhang, Sun et al., 2018). Finally, all of the former researches used a constant T_c without taking into account the bending-reduced T_c . Recent observation suggests that T_c may decrease widely close to trench by 25–75% due to normal faulting and serpentinization (Zhang, Lin et al., 2018). T_c in our model is therefore set to be a variable and the reduction in T_c indicates the area of plastic deformation after yielding (Figure 2a and Figure S3d in Supporting Information S1).

5.2. Effects of Surface Loading and Buoyancy on Plate Bending

From subduction (south) to collision (north) zone along the northernmost Manila trench, the increase in T_c indicates that the continent plate is more difficult to bend. Seismic profiles show that the deflection of the continental plate is greater than that of oceanic plate (Figures 1 and 2), implying that a greater loading is required at the collision zone. The M_0 and V_0 have the similar trend along the Manila trench and both require negative values (upward M_0 and V_0) at $\sim 21^\circ 30'$ N if we want to fit the profile T2 and T2933 at the same time (Figure 2a and 2b). Otherwise, the plate along profile T2 would be pulled down by the lateral force coming from the profile T2933. Figure 2b shows that without the upward M_0 and V_0 at $\sim 21^\circ 30'$ N, the variation of bending depth along the Manila trench is more smooth and inconsistent with observations (especially the profile T2 and T2933). Previous researches suggested that the upward bending might be caused by the buoyancy force resulting from the subduction of the light continental lithosphere (Chen et al., 2004; Lin, 2009) or the break-off of the leading edge part (Wang & Lee, 2011), while seismic data didn't show evidence of leading edge part break-off (Lo et al., 2017). Another possibility is the upward dragging of the buoyant continent on the northern part caused by the variation of subducting plate attribution from oceanic to the continental crust. To test this hypothesis, we designed a simple model to discuss the respective contributions of surface loading and the buoyancy (Figure 4a). The overriding wedge with thickness H_o was simplified to a triangle (Similar to the work of Lamb, 2006) (Figure 3a). If the difference of H_o from subduction to collision is ΔH_o , then the surface loading difference ΔQ is described by:

$$\Delta Q = \rho_o g \times \frac{\Delta H_o \times (\Delta H_o - d_t)}{\tan \theta} \quad (4)$$

where d_t is the margin relief and ρ_o is the average density of the overriding wedge (2300 kg/m³) (Please see Figure 3a). For the buoyancy, suppose the thickness of buoyant plate is 20 km and the crustal part changes northward from ~ 6 km thick oceanic (with density 3,000 kg/m³) to ~ 15 km continental crust (with density 2,700 kg/m³). Then the density contrast $\Delta \rho_b$ is ~ 240 kg/m³. Assume that the $\Delta \rho_b$ increase from 0 to 240 linearly, from the ocean to the continent. The buoyancy of the plate is given by:

$$\Delta F_b = \Delta \rho_b g \times \frac{\Delta H_o - d_t}{\sin \theta} \times T \quad (5)$$

in which the T is the thickness of buoyant plate. According to the Equations 4 and 5, we can estimate the variations of ΔF_b , ΔQ and the ration of $\Delta F_b/\Delta Q$ (Figure 4c). It shows that from the subduction to collision (oceanic to continental subducting plate), both surface loading and buoyancy increase and the increase of ΔF_b is faster at first, then slower than that of ΔQ . It causes that the $\Delta F_b/\Delta Q$ increase first and then decrease, exceeding 1 near the distance of 80 km. This corresponds the area with upward M_0 and V_0 , implying that the buoyancy may be a reason to cause plate bend upward. We find that variations of the density contrast and the buoyant plate thickness could change the absolute value of the $\Delta F_b/\Delta Q$, without changing the trend.

5.3. Bending Stress and Seismicity

We calculate the maximum principal bending stress and investigate the distribution of seismicity in the study area (Figures 3b–3e). It shows that the high seismicity zone at a depth of 35–50 km is occurring southwest of Taiwan Island (the blue ellipses in Figure 3). Figure 3 suggests that these concentrated earthquakes are intraplate events. They are perfectly located where the bending stress reaches the maximum and at the transition zone where the surface loading changes from accretionary wedge to mountain belt (Figure 3b). The focal mechanisms show

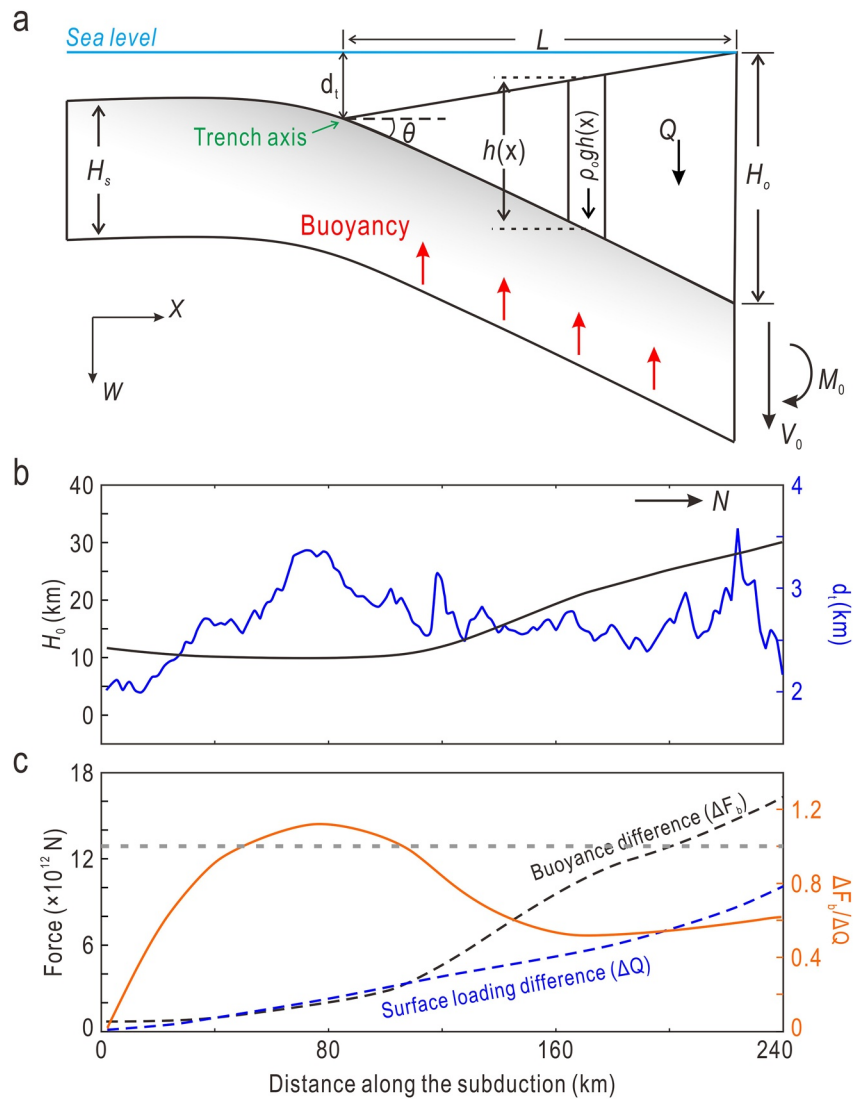


Figure 4. The simple model to investigate the separate contributions of surface loading from the overriding wedge and the buoyancy. (a) The sketch map of the model. (b) Variations of thickness of the overriding wedge (H_o) and the marginal relief (d_t) along the subduction zone. (c) Variations of ΔF_b , ΔQ and the ration of $\Delta F_b/\Delta Q$ along the subduction zone.

a complex stress field at the subduction-collision zone (Figures 3b–3e). The results show that most intraplate normal earthquakes occur in the shallow part (extensional region) of the subducting plate, while some strike-slip earthquakes occur near the neutral plane of the plate (Figures 3c and 3e). Lay et al. (2018) suggested that the strike-slip events in outer rise required laterally varying plate boundary conditions. We speculate that the intraplate strike-slip earthquakes may be caused by the 3-D effects of the along-strike variation of horizontal force. The bending stress also coincides with earthquakes distributed in the outer-rise region of the IOS (Figure 3d).

We proposed a model to illustrate the mechanism of plate bending from subduction to collision zone (Figure 5). At subduction zone, the deep slab pull caused plate bending and bending-related outer-rise earthquakes. However at the collision zone, the combination action of surface loading coming from the orogeny and the buoyancy will play important roles in plate bending. The huge plate deflection cause by the interaction between the upper and subducting plate may result in intense intraplate seismicity (Figure 5).

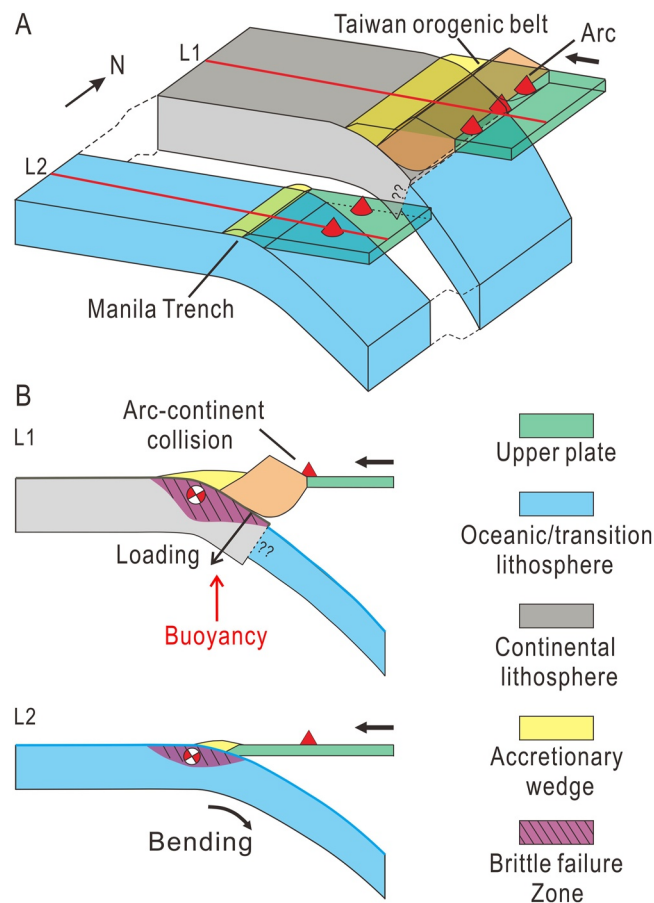


Figure 5. Model of plate bending from the subduction to the collision zone along the northern Manila trench.

6. Conclusion

From subduction to collision zone, both the loading and the T_c of the subducted plate have changed. Along the north Manila trench, the increase bending depth comes from the trade-off different loadings and the T_c of the subducted plate. Our flexural models show that both orogen and boundary loading plays important roles on bending of plate. We find that using a 3D elastic plate to model the flexural morphology requires an upward vertical force at the edge of the plate between $21^{\circ}30' N$ and $22^{\circ} N$. This upward force may come from lateral dragging of plate due to density contrast between oceanic and continental plate. The combined action of orogen loading and buoyancy created special plate geometry, leading to concentration of the bending stress and plastic deformation of the subducting plate at the transition zone from the subduction to collision. The plastic deformation corresponds to the concentrated of intraplate seismic at the depth of 35–50 km at southwest of the Taiwan.

Data Availability Statement

Data were not used, nor created for this research.

References

- Bowin, C., Lu, R. S., Lee, C. S., & Schouten, H. (1978). Plate convergence and accretion in Taiwan-Luzon region. *AAPG Bulletin*, 62, 1645–1672.
- Chang, J. H., Yu, H. S., Hsu, H. H., & Liu, C. S. (2012). Forebulge migration in late cenozoic Western Taiwan Foreland Basin. *Tectonophysics*, 578, 117–125. <https://doi.org/10.1016/j.tecto.2011.09.007>
- Chang, J. H., Yu, H. S., Lee, T. Y., Hsu, H. H., Liu, C. S., & Tsai, Y. T. (2012). Characteristics of the outer rise seaward of the Manila trench and implications in Taiwan–Luzon convergent belt, South China Sea. *Marine Geophysical Researches*, 33(4), 351–367. <https://doi.org/10.1007/s11001-013-9168-6>

Acknowledgments

This research is funded by the Guangdong Special Support talent team Program (2019BT02H594), the National Science Foundation of China grants (No. 41976064, 92158205, 91958211, 41706056, and 41890813), Hong Kong Research Grant Council Grants (No. 14304820, 14306119), the Award from CORE (a joint research center for ocean research between QNLM and HKUST), the Chinese Academy of Sciences grants Y4SL021001, QYZDY-SSW-DQC005, and 133244KYSB20180029; Southern Marine Science and Engineering Guangdong Laboratory (Guangzhou) grants GML2019ZD0205; and the National Key Research and Development Program of China grants 2018YFC0309800 and 2018YFC0310100.

- Chen, P. F., Bina, C. R., & Okal, E. A. (2004). A global survey of stress orientations in subducting slabs as revealed by intermediate-depth earthquakes. *Geophysical Journal International*, *159*(2), 721–733. <https://doi.org/10.1111/j.1365-246x.2004.02450.x>
- Chou, Y. W., & Yu, H. S. (2002). Structural expressions of flexural extension in the arc-continent collisional foredeep of western Taiwan. In T. B. Byrne & C.-S. Liu (Eds.), *Geology and Geophysics of an Arc-Continent Collision, Taiwan: Boulder, Colorado* (Vol. 358, pp. 1–12). Geological Society of America Special Paper.
- Contreras-Reyes, & E., & Osses, A. (2010). Lithospheric flexure modeling seaward of the Chile trench: Implications for oceanic plate weakening in the Trench Outer Rise region. *Geophysical Journal International*, *182*(1), 97–112.
- Eakin, D. H., McIntosh, K. D., Van Avendonk, H. J. A., Lavier, L., Lester, R., Liu, C. S., & Lee, C. S. (2014). Crustal-scale seismic profiles across the Manila subduction zone: The transition from intra-oceanic subduction to incipient collision. *Journal of Geophysical Research: Solid Earth*, *119*, 1–17. <https://doi.org/10.1002/2013JB010395>
- Garcia, E. S., Sandwell, D. T., & Bassett, D. (2019). Outer trench slope flexure and faulting at Pacific basin subduction zones. *Geophysical Journal International*. <https://doi.org/10.31223/osf.io/dbn8j>
- Govers, R., & Fichtner, A. (2016). Signature of slab fragmentation beneath Anatolia from full-waveform tomography. *Earth and Planetary Science Letters*, *450*, 10–19. <https://doi.org/10.1016/j.epsl.2016.06.014>
- Hayes, D. E., & Lewis, S. D. (1984). A geophysical study of the Manila trench, Luzon, Philippines: 1. Crustal structure, gravity, and regional tectonic evolution. *Journal of Geophysical Research*, *89*(B11), 9171–9195. <https://doi.org/10.1029/jb089ib11p09171>
- Huang, C. Y., Yuan, P. B., Lin, C. W., Wang, T. K., & Chang, C. P. (2000). Geodynamic processes of Taiwan arc-continent collision and comparison with analogs in Timor, Papua New Guinea, Urals and Corsica. *Tectonophysics*, *325*(1–2), 1–21. [https://doi.org/10.1016/S0040-1951\(00\)00128-1](https://doi.org/10.1016/S0040-1951(00)00128-1)
- Hunter, J., & Watts, A. B. (2016). Gravity anomalies, flexure, and mantle rheology seaward of circum-Pacific trenches. *Geophysical Journal International*, *207*(1), 288–316. <https://doi.org/10.1093/gji/ggw275>
- Judge, A. V., & McNutt, M. K. (1991). The relationship between plate curvature and elastic plate thickness: A study of the Peru-Chile trench. *Journal of Geophysical Research*, *96*(B10), 16625–16639. <https://doi.org/10.1029/90jb01772>
- Kuo-Chen, H., Wu, F. T., & Roecker, S. W. (2012). Three-dimensional P velocity structures of the lithosphere beneath Taiwan from the analysis of TAIGER and related seismic data sets. *Journal of Geophysical Research*, *117*, B06306. <https://doi.org/10.1029/2011jb009108>
- Lamb, S. (2006). Shear stresses on megathrusts: Implications for mountain building behind subduction zones. *Journal of Geophysical Research*, *111*, B07401. <https://doi.org/10.1029/2005jb003916>
- Lay, T., Ye, L., Bai, Y., Cheung, K. F., & Kanamori, H. (2018). The 2018 M_w 7.9 Gulf of Alaska earthquake: Multiple fault rupture in the Pacific plate. *Geophysical Research Letters*, *45*(18), 9542–9551. <https://doi.org/10.1029/2018gl079813>
- Lester, R., McIntosh, K., Van Avendonk, H. J. A., Lavier, L., Liu, C. S., & Wang, T. K. (2013). Crustal Accretion in the Manila trench accretionary wedge at the transition from subduction to mountain-building in Taiwan. *Earth and Planetary Science Letters*, *375*, 430–440. <https://doi.org/10.1016/j.epsl.2013.06.007>
- Levitt, D. A., & Sandwell, D. T. (1995). Lithospheric bending at subduction zones based on depth soundings and satellite gravity. *Journal of Geophysical Research*, *100*(B1), 379–400. <https://doi.org/10.1029/94jb02468>
- Liang, X., Sandvol, E., Chen, Y. J., Hearn, T., Ni, J., Klemperer, S., et al. (2012). A complex Tibetan upper mantle: A fragmented Indian slab and no south-verging subduction of Eurasian lithosphere. *Earth and Planetary Science Letters*, *333*, 101–111. <https://doi.org/10.1016/j.epsl.2012.03.036>
- Lin, A. T., & Watts, A. B. (2002). Origin of the West Taiwan basin by orogenic loading and flexure of a rifted continental margin. *Journal of Geophysical Research*, *107*, ETG2-1–ETG2-19. <https://doi.org/10.1029/2001JB000669>
- Lin, A. T., Watts, A. B., & Hesselbo, S. P. (2003). Cenozoic stratigraphy and subsidence history of the South China Sea margin in the Taiwan region. *Basin Research*, *15*(4), 453–478. <https://doi.org/10.1046/j.1365-2117.2003.00215.x>
- Lin, C.-H. (2009). Compelling evidence of an aseismic slab beneath central Taiwan from a dense linear seismic array. *Tectonophysics*, *466*(3–4), 205–212. <https://doi.org/10.1016/j.tecto.2007.11.029>
- Lo, C. L., Doo, W. B., Chen, H. K., & Hsu, S. K. (2017). Plate coupling across the northern Manila subduction zone deduced from mantle lithosphere buoyancy. *Physics of the Earth and Planetary Interiors*, *273*, 50–54. <https://doi.org/10.1016/j.pepi.2017.10.001>
- Ludwig, W. J., Hayes, D. E., & Ewing, J. I. (1967). The Manila trench and west Luzon trough—I. Bathymetry and sediment distribution. *Deep-Sea Research*, *14*(5), 533–544. [https://doi.org/10.1016/0011-7471\(67\)90063-0](https://doi.org/10.1016/0011-7471(67)90063-0)
- McIntosh, K., Nakamura, Y., Wang, T. K., Shih, R. C., Chen, A., & Liu, C. S. (2005). Crustal-scale seismic profiles across Taiwan and the western Philippine Sea. *Tectonophysics*, *401*(1–2), 23–54. <https://doi.org/10.1016/j.tecto.2005.02.015>
- McIntosh, K., van Avendonk, H., Lavier, L., Lester, W. R., Eakin, D., Wu, F., et al. (2013). Inversion of a hyper-extended rifted margin in the southern Central Range of Taiwan. *Geology*, *41*(8), 871–874. <https://doi.org/10.1130/g34402.1>
- Mouthereau, F., & Petit, C. (2003). Rheology and strength of the Eurasian continental lithosphere in the foreland of the Taiwan collision belt: Constraints from seismicity, flexure, and structural styles. *Journal of Geophysical Research*, *108*, 2512. <https://doi.org/10.1029/2002JB002098>
- Rangin, C., Le Pichon, X., Mazzotti, S., Pubellier, M., Chamot-Rooke, N., Aurelio, M., et al. (1999). Plate convergence measured by GPS across the Sundaland/Philippine Sea Plate deformed boundary: The Philippines and eastern Indonesia. *Geophysical Journal International*, *139*(2), 296–316. <https://doi.org/10.1046/j.1365-246x.1999.00969.x>
- Seno, T., Stein, S., & Gripp, A. E. (1993). A model for the motion of the Philippine Sea plate consistent with NUVEL-I and geologic data. *Journal of Geophysical Research*, *98*(B10), 17941–17948. <https://doi.org/10.1029/93JB00782>
- Shi, Y. H., & Eberhart, R. C. (1998). A modified particle swarm optimizer. *Proceeding of the IEEE International Conference on Evolutionary Computation*, 69–73.
- Silver, E. A., Reed, D., McCaffrey, R., & Joydowiryo, Y. (1983). Back arc thrusting in the Eastern Sunda Arc, Indonesia: A consequence of arc-continent collision. *Journal of Geophysical Research*, *88*(B9), 7429–7448. <https://doi.org/10.1029/JB088iB09p07429>
- Taylor, B., & Hayes, D. E. (1983). Origin and history of the South China Sea basin. In D. E. Hayes (Eds.), *The Tectonic and Geologic Evolution of Southeast Asian Seas and Islands: Part 2, Geophysical Monograph Series* (Vol. 27, pp. 23–56). AGU. <https://doi.org/10.1029/GM027p0023>
- Tensi, J., Mouthereau, F., & Lacombe, O. (2006). Lithospheric bulge in the west Taiwan Basin. *Basin Research*, *18*(3), 277–299. <https://doi.org/10.1111/j.1365-2117.2006.00296.x>
- Turcotte, D., & Schubert, G. (2014). *Geodynamics* (3rd ed., p. 626). Cambridge University Press.
- Van Avendonk, H. J. A., Kuo-Chen, H., McIntosh, K. D., Lavier, L. L., Okaya, D. A., Wu, F. T., et al. (2014). Deep crustal structure of an arc-continent collision: Constraints from seismic travel times in central Taiwan and the Philippine Sea. *Journal of Geophysical Research: Solid Earth*, *119*, 8397–8416. <https://doi.org/10.1002/2014jb011327>
- Wang, P., & Li, Q. (2009). Oceanographical and geological background. In P. Wang & Q. Li (Eds.), *The South China Sea* (pp. 25–73). Springer.

- Wang, W. H., & Lee, Y. H. (2011). 3-D plate interactions in central Taiwan: Insight from flexure and sandbox modeling. *Earth and Planetary Science Letters*, 308(1–2), 1–11. <https://doi.org/10.1016/j.epsl.2011.04.007>
- Watts, A. B. (2001). *Isostasy and flexure of the lithosphere* (p. 458). Cambridge University Press.
- Wolfe, J. A. (1988). Arc magmatism and mineralization in North Luzon and its relationship to subduction at the East Luzon and North Manila trenches. *Journal of Southeast Asian Earth Sciences*, 2, 79–93. [https://doi.org/10.1016/0743-9547\(88\)90011-6](https://doi.org/10.1016/0743-9547(88)90011-6)
- Yu, S. B., Kuo, L. C., Punongbayan, R. S., & Ramos, E. G. (1999). GPS observation of crustal deformation in the Taiwan-Luzon region. *Geophysical Research Letters*, 26(7), 923–926. <https://doi.org/10.1029/1999gl900148>
- Zhang, F., Lin, J., & Zhan, W. H. (2014). Variations in oceanic plate bending along the Mariana Trench. *Earth and Planetary Science Letters*, 401, 206–214. <https://doi.org/10.1016/j.epsl.2014.05.032>
- Zhang, F., Lin, J., Zhou, Z. Y., Yang, H. F., & Zhan, W. H. (2018). Intra- and intertrench variations in flexural bending of the Manila, Mariana and global trenches: Implications on plate weakening in controlling trench dynamics. *Geophysical Journal International*, 212(2), 1429–1449. <https://doi.org/10.1093/gji/ggx488>
- Zhang, J., Sun, Z., Xu, M., Yang, H., Zhang, Y., & Li, F. (2018). Lithospheric 3-D flexural modelling of subducted oceanic plate with variable effective elastic thickness along the Manila trench. *Geophysical Journal International*, 215(3), 2071–2092. <https://doi.org/10.1093/gji/ggy393>
- Zhang, J. Y., Zhang, F., Lin, J., & Yang, H. (2021). Yield failure of the subducting plate at the Mariana Trench. *Tectonophysics*, 814, 228944. <https://doi.org/10.1016/j.tecto.2021.228944>
- Zhou, Z. Y., Lin, J., Behn, M. D., & Olive, J. A. (2015). Mechanism for normal faulting in the subducting plate at the Mariana Trench. *Geophysical Research Letters*, 42(11), 4309–4317. <https://doi.org/10.1002/2015GL063917>